AIP | Journal of Applied Physics

Misalignment-free signal propagation in nanomagnet arrays and logic gates with 45°-clocking field

Zheng Li, Byung Seok Kwon, and Kannan M. Krishnan

Citation: Journal of Applied Physics **115**, 17E502 (2014); doi: 10.1063/1.4859996
View online: http://dx.doi.org/10.1063/1.4859996
View Table of Contents: http://scitation.aip.org/content/aip/journal/jap/115/17?ver=pdfcov
Published by the AIP Publishing

JOURNAL OF APPLIED PHYSICS **115**, 17E502 (2014)

Misalignment-free signal propagation in nanomagnet arrays and logic gates with 45°-clocking field

Zheng Li, Byung Seok Kwon, and Kannan M. Krishnan[a)]
Department of Materials Science and Engineering University of Washington, Box 352120, Seattle, Washington 98195, USA

(Presented 8 November 2013; received 10 September 2013; accepted 14 October 2013; published online 3 January 2014)

A key obstacle for the application of Magnetic Quantum-dot Cellular Automata (MQCA) is the misalignment of clocking field, which results in low stability for both signal propagations within nanomagnet array and logic operation in majority gates. Here, we demonstrate that a reversal clocking field applied at 45° off the hard axis, with progressively reduced amplitude, applied to a shape-tuned nanomagnet array fabricated by e-beam lithography, helps intrinsically eliminate the misalignment sensitivity of the elements and results in correct signal propagation. Further, least reversal steps and reduced field amplitude was required owing to the 45°-clocking field. This clocking field was also tested for majority gates (OR function) and characterized by Magnetic Force Microscopy demonstrating correct output. This novel design provides high stability for signal propagation and logic operation of MQCA and potentially paves way for its application.
 [http://dx.doi.org/10.1063/1.4859996]

While magnetic material has been widely used for information storage for some time, recently attempts have been made to exploit magnetic phenomena for logic functionality using different lithographically defined nanostructures.[1,2] Among them is the concept of Magnetic Quantum-dot Cellular Automata (MQCA)[3] aiming to process information and perform Boolean logic operations via nearest-neighbor dipole coupling in a coordinative arrangement. A key function of MQCA is signal propagation in a nanomagnet array, for which a clocking field is required. Traditionally, the clocking field is applied along the nanomagnet hard-axis to realize a "NULL" state.[3,4] However, a fabrication misalignment is inevitable, which makes such MQCA logic practically challenging: field misalignment of $\pm 1°$ would lead to incorrect logic operation 75% of the time.[3]

To overcome this limitation, many approaches have been tested.[4–7] In particular, we proposed a novel configuration[8] where a reversal clocking field with progressively reduced amplitude was applied to a shape-tuned nanomagnet array. It helps enforce correct signal propagation against field misalignment up to 5°, demonstrating cascade-like signal propagation. However, there are drawbacks to this configuration. The misalignment angle, θ, affects the amplitude of the clocking field; larger reversal field is required for a smaller θ. This property is intrinsically correlated to the angular dependence of the reversal field for a uniaxial anisotropic element and may result in redundant clocking process and slower signal propagation.

Here, we propose a misalignment-free configuration where the least number of field reversals with reduced amplitude is required for a wide range of θ. Specifically, a clocking field applied at 45° off the hard axis was designed by micromagnetic simulation and tested with lithographically fabricated elements and arrays. Correct signal propagation can be achieved within an array at both 42° and 45°-off the hard axis. In other words, clocking field with randomly distributed misalignment less than 3° would not block the correct signal propagation and the field is both more efficient and energy saving. Further, studies of majority gates for the OR logic operations show correct output. Experimentally, these configurations were fabricated by electron-beam lithography (EBL) and correct signal propagation and logic operations were confirmed by magnetic force microscopy (MFM).

Experimentally, we fabricated the nanomagnet arrays using EBL. Polymethyl-methacrylate (PMMA)/LOR 1A (MicroChem Corp., Newton, MA) bilayer resist was used for undercut profile.[9,10] A 20 nm-thick Fe, with a 3 nm-thick Au cap, was deposited using Ion Beam Sputtering with base pressure better than 5×10^{-8} Torr. The magnetic configurations were investigated by MFM with the magnetic field applied parallel to the sample surface using 15 nm CoCr coated low moment probes with a lift height of 50 nm.

The following parameters were used for all LLG micromagnetic simulations:[11] saturation magnetization, $M_S = 1000$ emu/cm^3, exchange stiffness, $A = 2.1\ \mu$erg/cm, magnetocrystalline anisotropy, $K_{mc} = 0$, for each of the $5 \times 5 \times 20$ nm^3 cells due to the polycrystalline structure of the nanomagnet arrays and thickness, $t = 20$ nm. We first considered two nanomagnets with aspect ratios of 2:1 (S_2) and 3:1 (S_3) [Fig. 1(a)]. If we define the domain wall energy $\gamma = 4\sqrt{AK_u}$ and single domain particle size $D_c = 1.4\gamma/M_S^2$, where A, K_U, and M_S are the exchange stiffness, uniaxial anisotropy, and saturation magnetization of the given material, then we can get $Dc_{(Fe)} = 60$ nm for Iron. Thus, for both elements, 100 nm in width, the reversal process is considered to be a coherent rotation of magnetization and best-described by the well-known Stoner-Wohlfarth model.[12] A reduced flipping field H_{fl} with minimum angular-sensitivity would be realized if the external field is applied 45° off the hard axis, which is related to the Stoner-Wohlfarth astroid.

a)Author to whom correspondence should be addressed. Electronic mail: kannanmk@uw.edu

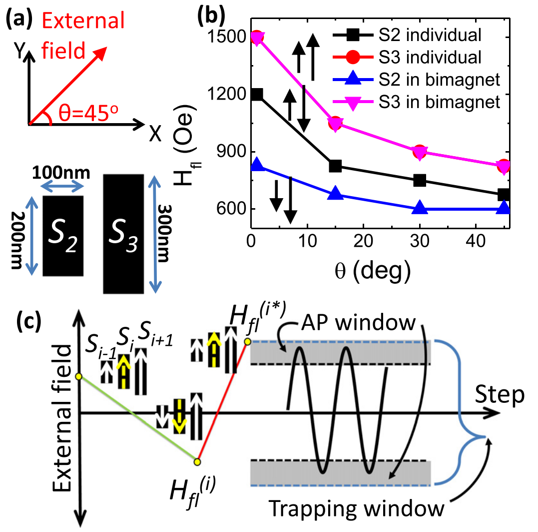

FIG. 1. (a) Schematic of the nanomagnet structure and the 45° clocking field. (b) The angular dependence of flipping field H_{fl} for elements S_2 and S_3. (c) The array magnetic state (only three elements shown here). S_i (highlighted with yellow dotted arrow) will flip to the AP-state with S_{i+1} within the AP-window; after that this AP-state will be stable within the Trapping-window.

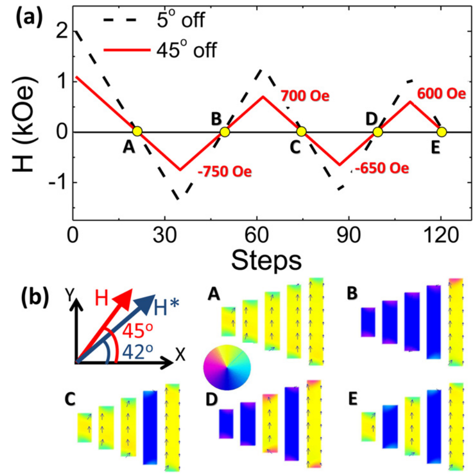

FIG. 2. (a) The 45° clocking field employed with progressively reduced amplitude. (b) Simulated magnetic states corresponding to different steps in (a). Both 42° and 45° offset with respect to the hard axis was tested.

First, we modeled both elements individually and the angular (θ)-dependence of H_{fl} followed the Stoner-Wohlfarth model for both elements [Fig. 1(b)] reaching its minimum at 45°, with the magnitude of H_{fl} proportional ($S_3 > S_2$) to its shape anisotropy, K_S. Next, to study the dipole interactions, we tested bimagnet system where S_2 and S_3 were placed adjacent to each other. Similarly, H_{fl} decreases with increasing θ. However, S_2 flips earlier owing to the dipole interaction where magnetic antiparallel state (AP-state) is energetically more favorable. In short, an external field applied 45° off the hard axis triggers S_2 flipping with smaller H_{fl}, which is also less θ-sensitive. Therefore, by applying and removing 45°-clocking field with amplitude between $H_{fl}^{(2)}$ and $H_{fl}^{(3)}$, we could realize AP-state with smaller field amplitude and higher θ tolerance. This AP-state corresponds to signal propagation in a nanomagnet array, while θ tolerance is related to misaligned clocking field.

Next, consider a nanomagnet array with the shape anisotropy, K_S, of each element progressively reduced by shortening its long axis. The 45°-clocking field was applied, which keeps reversing with progressively reduced amplitude. Any element S_i will keep flipping till the field amplitude is smaller than its energy barrier, which is related to its intrinsic anisotropy K_S and the dipole interactions from adjacent elements S_{i-1} and S_{i+1}. Elements with higher K_S will become magnetically stable first. Consider a specific element, S_i, as an example. Considering only dipole interaction from adjacent elements S_{i+1} and S_{i-1}, the magnetization of S_i will be more stable if it is aligned AP to both of them. As the field amplitude is reduced gradually, S_{i+1} will become magnetically stable first, facilitating S_i to realize an AP-state, as shown in Fig. 1(c). After that, it requires larger field $H_{fl}^{(i*)}$ for S_i to flip back since the parallel state (P-state) is energetically unfavorable. As a result, if the reversal field is within the AP-window with amplitude higher than $H_{fl}^{(i)}$ but lower than $H_{fl}^{(i*)}$, S_i will flip into the AP-state with respect to S_{i+1}. After that, if this reversal field is within the Trapping-window where amplitude is lower than $H_{fl}^{(i*)}$, it will be trapped in this state. In general, if the amplitude of the reversal clocking field is reduced progressively passing through $H_{fl}^{(i)}$ of each elements sequentially, the AP-state will be realized from the high anisotropic elements down to the lower ones, achieving unidirectional signal propagation. The higher the K_S of an element, the earlier it will become magnetically stable against the clocking field. More details about this process can be found elsewhere.[8]

To demonstrate this signal propagation, we modeled a chain of five rectangular elements, with the same short axis length (100 nm), and the long axis length varying from 600 nm to 200 nm corresponding to a gradually decreasing K_S. The same 45°-clocking field was applied [Fig. 2(a)] with progressively reduced amplitude from 750 Oe down to 600 Oe. The dotted line represents the field magnitude required when applied at 5° off the hard axis,[8] suggesting that almost halved field magnitude is required if applied 45° off the hard axis. Figure 2(b) shows the chain magnetic state corresponding to different steps in Fig. 2(a). Cascade-like signal propagation is observed.[8] Further, to test its misalignment tolerance, we simulated the field 42° off the hard axis. This 3° variation, corresponding to the typical fabrication misalignment, does not affect correct signal propagation. Thus, the 45°-clocking field configuration achieves smaller field and higher misalignment tolerance within an array, i.e., more reliable signal propagation and lower energy consumption.

To further test this configuration, we fabricated Fe nanomagnet arrays. A continuous magnetostatic reversal field, similar to the simulation [Fig. 2(a)] was applied and the evolution of magnetization flipping was observed to be the same as in the previous work[8] (not shown here). However, smaller field amplitude is required here for the 45° clocking field.

Next, we studied validity of this 45°-clocking field for logic operations when applied to majority gates. By setting one input [middle left in Fig. 3(b), for example] to a logic 0 (1), the majority gate can execute OR (AND) function. Different from the nanomagnet array, majority gates require coordinated rearrangement of the elements for both signal input and logic operation, which would weaken the dipole

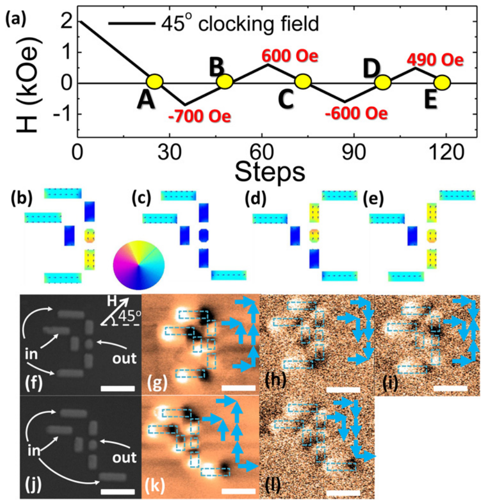

FIG. 3. (a) The 45° clocking field employed for logic operation. (b)-(e) The simulation results of all four majority gates. (f) and (j) SEM images of lithographically patterned OR gates (only two are demonstrated here), with the magnetic state evolution observed by MFM shown on the right (g)-(i) and (k)-(l), respectively. The magnetic direction is defined as "from white to black" while the arrows serve for visual guidance. The scale bar stands for 500 nm in (f)-(l).

coupling between elements and requires accurate field tuning down to tens of Oersteds, as discussed below. The reversal field with amplitude decreasing from 700 Oe down to 490 Oe [Fig. 3(a)] was used to simulate all four input combinations for the OR gate, with the bit value = 0(1) assigned to magnetization direction down (up) along the easy axis for two vertical inputs (above and below) and the center output. The final stage is shown in Figs. 3(b)–3(e), suggesting correct logic operation under 45° clocking field. Further, Figs. 3(f) and 3(j) show SEM images of two gates fabricated for logic operation test. The MFM images on the right are the magnetic evolution corresponding to stage A–C in Fig. 3(a). Even though correct logic operation is achieved by only two reversals, the complete clocking field in Fig. 3(a) is required for all four input combinations ensuring that the output element finds its ground state. In summary, the 45°-clocking reversal field was demonstrated to facilitate logic operations for majority gates.

Finally, we would like to discuss the feasibility of this 45°-clocking field. The key advantage this configuration has over the traditional clocking field is the misalignment-free mechanism. It was estimated[13] that the misalignment angle θ should satisfy $\tan\theta < (H_C^{easy}/H_C^{hard}) \ll 1$ for traditional clocking fields applied along the hard axis, where H_C^{easy} and H_C^{hard} represents the fields required to magnetize the element along the easy and hard axis, respectively. This highly accurate directionality is practically challenging. Even though the hard-axis reversal clocking field[8] partly addressed this issue for nanomagnet arrays, the redundant clocking process and slower signal propagation is still undesirable. The 45°-clocking field solves this problem intrinsically by applying the field along the angular-insensitive direction of 45° with respect to the hard axis. Furthermore, the reduced field amplitude is more efficient and energy saving. Next, for proper functioning of majority gates, accurate field tuning down to tens of Oersteds is required since the dipole coupling is weakened when the elements are not aligned parallel along each other affecting the corresponding energy ground state. This is a general problem for most architecture other than the nanomagnet arrays. However, it is feasible since the magnitude of the current generating the clocking field can be controlled with a much better accuracy. To generate a magnetic field $\sim 5 \times 10^3$ Oe along the top surface of the copper wires, a current density $\sim 10^6$ A/cm^2 is required.[14] Considering a normal current generator[15] with capacity of 500 A and step of 0.2 A, this field could be achieved since the accuracy is better than 400 A/cm^2, or 2 Oe. Thus, our design is practically applicable. One of the drawbacks of this configuration is that it requires N-times field reversal for signal to propagate down an array with N-elements. Thus, it is reasonable to break a long chain down to several short ones, which are connected by a granular clocking field. Since the signal propagates unidirectionally from higher anisotropic element to lower ones, signal refreshment from lower to higher ones is required. This could be achieved by a granular clocking scheme where a local field is applied individually to the output element alone.[13] Demanding much elaborate fabrication, this granular clocking field may only be used for signal refreshment. Finally, to implement the proposed architecture into a full circuit, a local clocking field is required, which is normally generated by copper wires embedded underneath. The wire current should be perpendicular to the 45° clocking field and confined within a local area ($\sim 1.5\,\mu$m $\times$ 1.5 μm). This copper wire can be realized through the standard fabrication process.[16] A thicker wire with high aspect-ratio sidewalls, combined with high-permeability claddings (such as supermalloy),[17] would help retain the reluctance and reduce the power consumption as well.

This work was supported by NSF-DMR under Grant No. 1063489. Part of this work was conducted at the University of Washington NanoTech User Facility, a member of the NSF National Nanotechnology Infrastructure Network (NNIN). Z.L. would like to acknowledge China Scholarship Council (CSC) for partial financial support.

[1]D. A. Allwood *et al.*, Science **309**, 1688 (2005).
[2]S. S. P. Parkin *et al.*, Science **320**, 190 (2008).
[3]A. Imre *et al.*, Science **311**, 205 (2006).
[4]M. T. Niemier *et al.*, IEEE Trans. Nanotechnol. **11**, 220 (2012).
[5]T. Hesjedal and T. Phung, Appl. Phys. Lett. **96**, 072501 (2010).
[6]D. B. Carlton *et al.*, Nano Lett. **8**, 4173 (2008).
[7]B. Lambson *et al.*, Appl. Phys. Lett. **100**, 152406 (2012).
[8]Z. Li and K. M. Krishnan, J. Appl. Phys. **113**, 17B901 (2013).
[9]W. Zhang *et al.*, J. Micromech. Microeng. **21**, 045024 (2011).
[10]W. Zhang *et al.*, J. Appl. Phys. **107**, 09D724 (2010).
[11]M. R. Scheinfein, LLG Micromagnetics Simulator™.
[12]E. C. Stoner and E. P. Wohlfarth, Philos. Trans. R. Soc. A: Phys., Mathemat. and Eng. Scie. **240**, 599 (1948).
[13]S. Bandyopadhyay and M. Cahay, Nanotechnology **20**, 412001 (2009).
[14]M. T. Niemier *et al.*, "Clocking structures and power analysis for nanomagnet-based logic devices," in *Proceedings of the International Symposium on Low Power Electronics and Design* (2007), p. 26.
[15]See http://www.avtechpulse.com/ for information about general purpose pulse generators.
[16]M. T. Alam *et al.*, IEEE Trans. Nanotechnol. **9**, 348 (2010).
[17]X. Yang *et al.*, Microelec. J. **43**, 386 (2012).